Surface tension and density of binary lead and lead-free Sn-based solders

2005 J. Phys.: Condens. Matter 17 7867

(http://iopscience.iop.org/0953-8984/17/50/007)

INSTITUTE OF PHYSICS PUBLISHING JOURNAL OF PHYSICS: CONDENSED MATTER

J. Phys.: Condens. Matter **17** (2005) 7867–7873 doi:10.1088/0953-8984/17/50/007

Surface tension and density of binary lead and lead-free Sn-based solders

I Kaban[1,3], S Mhiaoui[2], W Hoyer[1] and J-G Gasser[2]

[1] Institute of Physics, Chemnitz University of Technology, D-09107 Chemnitz, Germany
[2] Laboratoire de Physique Milieux Denses, Universite de Metz, 1 Boulevard Arago, 57078 Metz Cedex 3, France

E-mail: ivan.kaban@physik.tu-chemnitz.de

Received 25 July 2005, in final form 25 September 2005
Published 2 December 2005
Online at stacks.iop.org/JPhysCM/17/7867

Abstract

The surface tension and density of the liquid $Sn_{60}Pb_{40}$, $Sn_{90}Pb_{10}$, $Sn_{96.5}Ag_{3.5}$ and $Sn_{97}Cu_3$ solder alloys (wt%) have been determined experimentally over a wide temperature interval. It is established that the surface tension of liquid $Sn_{90}Pb_{10}$ is about 7% higher than that of a traditional $Sn_{60}Pb_{40}$ solder and that the surface tension of $Sn_{96.5}Ag_{3.5}$ and $Sn_{97}Cu_3$ alloys is about 12% higher than that of $Sn_{60}Pb_{40}$. The analytical expressions for the temperature dependences of the surface tension and density are given.

1. Introduction

In accordance with the Directives of the European Parliament and of the Council *on 'waste electrical and electronic equipment'* and *on 'restriction of use of certain hazardous substances'*, lead will be banned from production of new electrical and electronic devices from 1 July 2006 [1]. The traditional lead–tin solders have to be replaced with new solders, free of lead. Other alloys with a melting temperature close to the commonly used Sn–Pb eutectic and having appropriate properties should be found. For industrial usage of a new soldering material its physical properties (electrical, chemical, thermal, mechanical etc) in the solid as well as in the liquid state should be well known. Therefore many potential candidates for lead-free solders are being intensively studied in various laboratories.

Among the most important physical properties and phenomena playing a crucial role in the soldering process are the surface tension and the wetting behaviour of the solder. In this work we study the surface tension of liquid $Sn_{96.5}Ag_{3.5}$, $Sn_{97}Cu_3$, $Sn_{90}Pb_{10}$ in comparison with the surface tension of the classical solder $Sn_{60}Pb_{40}$ (here and further all compositions are given in weight per cent). The densities of the alloys investigated are also reported.

[3] Author to whom any correspondence should be addressed.

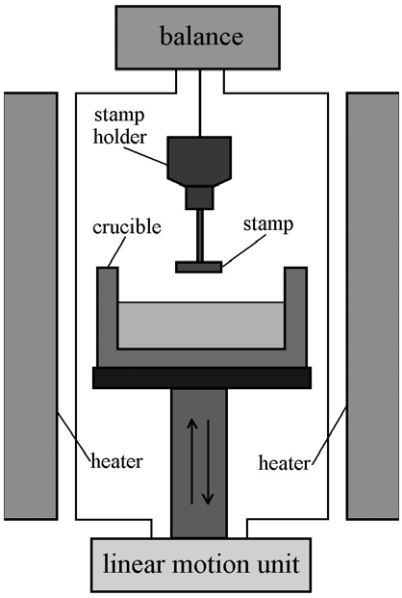

Figure 1. Scheme of the tensiometer.

2. Measurement technique

2.1. Surface tension determination

The surface tension of liquid alloys was determined with a tensiometric method described in detail in [2, 3]. The principles of the experimental set-up and measuring process are shown schematically in figures 1 and 2. The technique is based on the experimental measurement of the force exerted on the alumina stamp submerged below the level of the free liquid surface. It is noteworthy that in this method a complete set of experimental data (force as a function of the stamp height) are analysed, and not just a maximum force. The stamp's form, as shown in figure 2, allows the investigation of meniscus formation and contraction up to the complete tearing of the stamp away from the surface. Thus, the force of interaction of the stamp with the liquid sample $F^{\exp}$ is determined as a function of the stamp's height h with respect to the position of the crucible.

As an example, the experimental curve for liquid $Sn_{96.5}Ag_{3.5}$ at 550 °C is shown in figure 2. The force $\vec{F}^{\exp}$ measured with the balance initially set to zero is the resultant of the Archimedes buoyancy force $\vec{F}_{\mathrm{A}}$ and the force caused by the meniscus $\vec{F}_{\mathrm{Men}}$:

$$\vec{F}^{\exp} = \vec{F}_{\mathrm{A}} + \vec{F}_{\mathrm{Men}}. \tag{1}$$

The buoyancy force equals

$$F_{\mathrm{A}} = \Delta\rho g V_{\mathrm{A}} \tag{2}$$

where V_{A} is the volume of the stamp submerged into the melt, g is the gravitational acceleration, $\Delta\rho = \rho - \rho_{\mathrm{v}}$ is the density difference between the liquid phase (ρ) and the vapour phase (ρ_{v}).

The force caused by the meniscus can be expressed on the one hand through the contact angle Θ by the equation:

$$F_{\mathrm{Men}} = \sigma 2\pi r_{\mathrm{s}} \cos\Theta \tag{3}$$

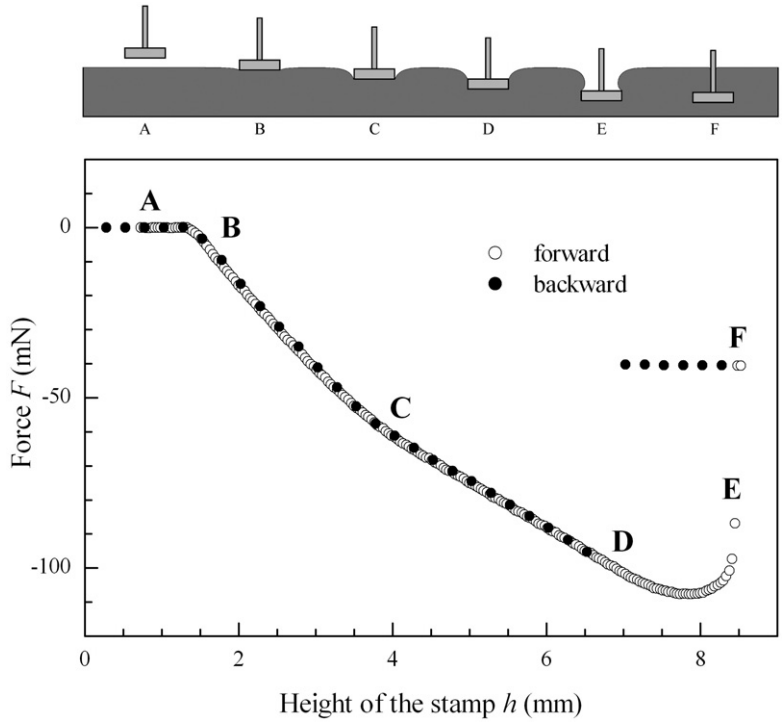

Figure 2. The main stages of the measuring process and the experimental curve for liquid $Sn_{96.5}Ag_{3.5}$ at 500 °C. (A) The stamp is above the liquid. (B) The stamp touches the liquid and the meniscus is formed; the buoyancy force and the force of surface tension act on the stamp. (C–D) The stamp is further submerged into the liquid; the measured force depends linearly on the stamp's position (buoyancy). (D) The contact line reaches the upper edge of the stamp; the necking of the meniscus starts. (E) The stamp is ready to tear away from the surface. (F) The meniscus is broken.

where σ is the surface tension and r_s is the radius of the stamp. On the other hand, the force on the part of surface acting on the stamp in the vertical direction is equal to the weight of the meniscus with volume V_{Men}:

$$F_{Men} = \Delta\rho g V_{Men}. \tag{4}$$

The relation between the shape of the meniscus and the force exerted by the meniscus on the stamp underlies the basis of the applied measurement technique.

Thus the volume of the meniscus can be calculated with equation (4) if the buoyancy and geometry of the crucible and of the stamp are taken into account. After transformation of coordinates, the volume of the meniscus V_{Men}^{exp} is determined as a function of the height of the contact line x_0. This transformation is performed for the subsequent comparison of the experimental meniscus volume $V_{Men}^{exp}(x_0)$ with the modelled volumes $V_{Men}^{model}(x_0)$ in the same coordinates.

The meniscus is modelled by the numerical solution of the Laplace equation of capillarity, which describes the pressure difference Δp across the curved liquid–vapour interface:

$$\sigma\left(\frac{1}{R_1} + \frac{1}{R_2}\right) = \Delta p = p_1 - p_2, \tag{5}$$

where R_1 and R_2 are the principal radii of curvature of the interface; p_1 and p_2 are, respectively, the pressure on the concave and the convex sides of the meniscus. Owing to the cylindrical

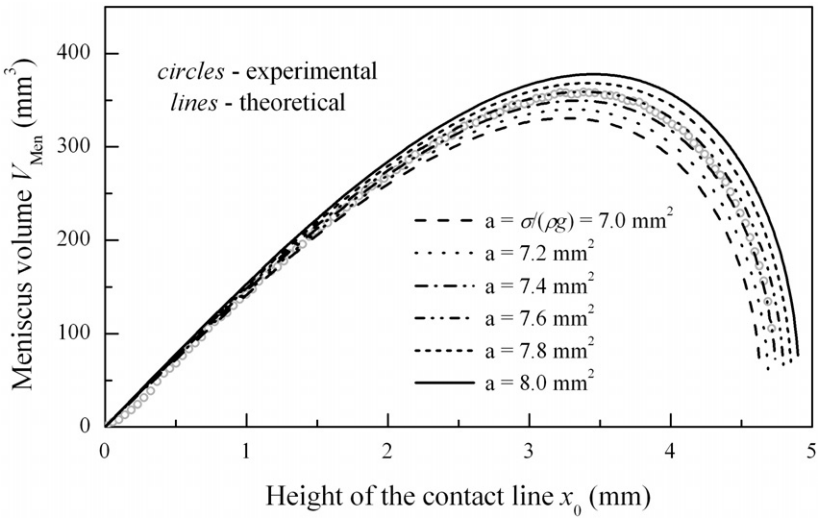

Figure 3. The experimental meniscus volume curve for the liquid $Sn_{96.5}Ag_{3.5}$ at 550 °C compared to the volume curves modelled for various capillary constants.

form of the stamp, the solution of equation (5) is reduced to a one-dimensional problem, so the Laplace equation contains the curvature radii and a linear gravitation component:

$$\sigma\left(\frac{1}{R_1}+\frac{1}{R_2}\right)=\Delta\rho g x, \tag{6}$$

where x is a coordinate in the direction of the gravitation force (i.e. along the axis of symmetry). Replacing the principal radii of curvature by the differential geometry expressions, one obtains the following equation [2–5]:

$$\frac{x'}{r(1+x'^2)^{1/2}}+\frac{x''}{(1+x'^2)^{3/2}}=\frac{\Delta\rho g x}{\sigma}, \tag{7}$$

where r is the radial distance in a horizontal plane from the axis of symmetry ($r^2=y^2+z^2$), $x'=\mathrm{d}x/\mathrm{d}r$, $x''=\mathrm{d}^2x/\mathrm{d}r^2$.

The numerical solution of equation (7) allows modelling of the radial–symmetrical meniscus and calculation of the dependence of its volume on the height of the contact line $x_0-V_{\mathrm{Men}}^{\mathrm{model}}(x_0)$, for different radii of the contact line (i.e. for different stamps) and for various values of the capillary constant a, which is defined as

$$a=\frac{\sigma}{\Delta\rho g}\simeq\frac{\sigma}{\rho g} \tag{8}$$

since the vapour phase density can be neglected.

Comparison of the experimental volume curves $V_{\mathrm{Men}}^{\mathrm{exp}}(x_0)$ with the volumes of menisci modelled for the size of the stamp used $V_{\mathrm{Men}}^{\mathrm{model}}(x_0)$ results in the determination of the capillary constant for the liquid studied, as shown for example in figure 3. The surface tension can be calculated from the capillary constant a with equation (8) when the density of the liquid is known.

2.2. Density determination

It is an advantage of the measurement technique that the density of a liquid being studied can be found from the same experimental data as are used for the determination of the capillary

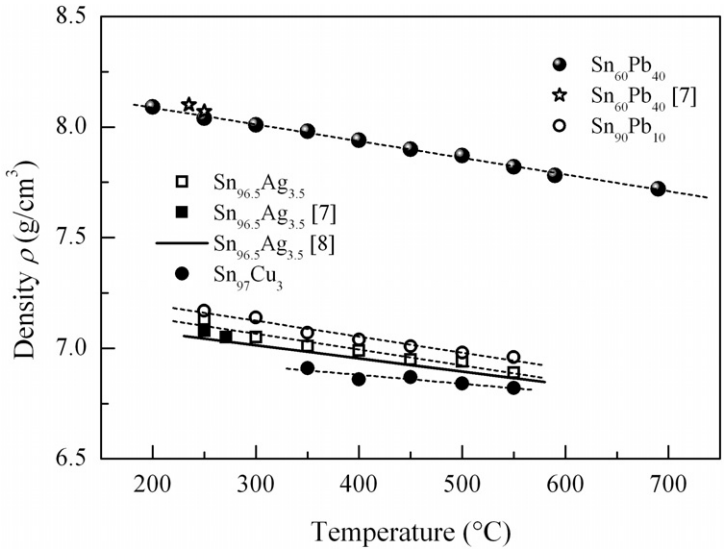

Figure 4. The temperature dependences of the density in the liquid alloys studied. The dashed lines are the linear fits (see table 1 for details).

constant. It is assumed that the shape of the meniscus and the surface tension are constant when the liquid surface moves along the cylindrical stamp (stages (C)–(D) in figure 2). At this stage, only the buoyancy force exerted by the liquid on the stamp immersed into it changes. Thus, from the linear part of the experimental curve, the variation of the measured force $F^{\exp}$ with the height $h - \mathrm{d}F^{\exp}/\mathrm{d}h$ can be determined. Then the density of the liquid can be calculated using the expression

$$\rho = \frac{\mathrm{d}F^{\exp}}{\mathrm{d}h}\frac{1}{g\pi}\left(\frac{1}{r_{\mathrm{s}}^2} - \frac{1}{R_{\mathrm{t}}^2}\right) \tag{9}$$

where R_{t} and r_{s} are the radii of the crucible and stamp, respectively. The experimental density is represented in figure 4.

3. Experimental details

Industrial lead-free solders $Sn_{96.5}Ag_{3.5}$, $Sn_{97}Cu_3$, $Sn_{90}Pb_{10}$ (Stoop n.v., a member of Fenix Metals) and $Sn_{60}Pb_{40}$ alloy prepared from pure Sn (99.99%) and Pb (99.999%) were used for the investigations.

The measurements have been performed in the tensiometer shown schematically in figure 1. Before heating, the chamber was evacuated to better than 5×10^{-5} mbar and then filled with a gas mixture of Ar–10 % H_2 with a total pressure of $\sim$1 bar. Additionally a niobium getter was used to reduce the amount of oxygen that gets into the chamber through leaks during measurements. The heating system consisted of a concentric Kanthal heater outside the chamber, a power supply and an electronic temperature control device. The graphite crucible (5 cm inner diameter, 4 cm height) was moved by an ultrahigh vacuum manipulating system. The diameter of the working part of the alumina stamp was 15 mm and its height was 3 mm. The force exerted on the stamp was measured by a balance with an accuracy of 1 mg. The experimental error did not exceed $\pm 3\%$ for the surface tension and $\pm 1.5\%$ for the density.

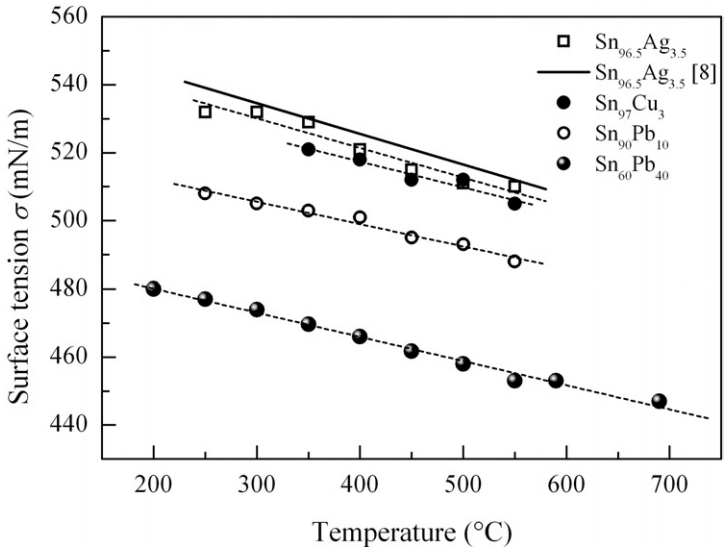

Figure 5. The temperature dependences of the surface tension for the liquid alloys studied. The dashed lines are the linear fits (see table 1 for details).

4. Results and discussion

Experimental curves similar to those shown in figure 2 have been obtained for all alloys investigated. It is noteworthy that the forward and backward curves were smooth and coincided. The meniscus volumes $V_{\mathrm{Men}}^{\mathrm{exp}}(x_0)$ were calculated from the experimental data and compared with the respective simulated functions $V_{\mathrm{Men}}^{\mathrm{model}}(x_0)$. From the comparison, the capillary constants were determined. Then the surface tension of the alloys studied was calculated with equation (8) using the capillary constants and experimentally determined densities.

Figures 4 and 5 show the temperature dependences of the density and surface tension for the alloys studied. As one can see, both the surface tension and density decrease with increasing temperature. Obviously one can accept linear temperature dependences in the temperature intervals investigated. Therefore, for convenience of practical use the experimental values of σ and ρ were fitted with the linear functions $\sigma(T) = \sigma_0 - \frac{\mathrm{d}\sigma}{\mathrm{d}T}T$ and $\rho(T) = \rho_0 - \frac{\mathrm{d}\rho}{\mathrm{d}T}T$ (T is the absolute temperature). The parameters σ_0 and ρ_0, the temperature coefficients $\mathrm{d}\sigma/\mathrm{d}T$ and $\mathrm{d}\rho/\mathrm{d}T$, and the errors of the fits are given in table 1. For comparison, the respective data for liquid Sn taken from [6] are presented in table 1.

The experimental results show that the surface tension of liquid $Sn_{96.5}Ag_{3.5}$, $Sn_{97}Cu_3$ and $Sn_{90}Pb_{10}$ is higher than that of a traditional $Sn_{60}Pb_{40}$ solder. For example, at 250 °C $\sigma(Sn_{60}Pb_{40}) = 477$ mN m^{-1}, $\sigma(Sn_{90}Pb_{10}) = 508$ mN m^{-1}, $\sigma(Sn_{96.5}Ag_{3.5}) = 532$ mN m^{-1}, and at 350 °C $\sigma(Sn_{97}Cu_3) = 521$ mN m^{-1}.

The very good agreement between the absolute values of the density for liquid $Sn_{98.5}Ag_{3.5}$ and $Sn_{60}Pb_{40}$ obtained in the present work and the published data [7, 8] confirms the reliability of the method applied for density determination (see figure 4). The reliability of the surface tension measurements is proven by a coincidence within 1% of our results for liquid $Sn_{98.5}Ag_{3.5}$ and the recent data [8] (see figure 5). The surface tension of liquid $Sn_{60}Pb_{40}$ measured by us (480 mN m^{-1} at 200 °C) lies in a middle of the values from other works [9–12]. For example, $\sigma(Sn_{60}Pb_{40}) \approx 507$ mN m^{-1} has been obtained at 215 °C [11] and $\sigma(Sn_{65}Pb_{35}) \approx 461$ mN m^{-1} at 200 °C [12]).

Table 1. The temperature dependences of the surface tension $\sigma(T)$ and the density $\rho(T)$ for the liquid alloys studied: the linear fits to the experimental data. The data for pure Sn are taken from [6].

Composition (wt%)	$\sigma(T) = \sigma_0 - \frac{d\sigma}{dT}T$ (mN m^{-1})		$\rho(T) = \rho_0 - \frac{d\rho}{dT}T$ (g cm^{-3})	
	σ_0 (mN m^{-1})	$\frac{d\sigma}{dT}$ (10^{-2} mN m^{-1} K^{-1})	ρ_0 (g cm^{-3})	$\frac{d\rho}{dT}$ (10^{-4} g cm^{-3} K^{-1})
Sn	572 ± 3	7.6 ± 0.3	7.37 ± 0.06	8.2 ± 0.8
$Sn_{98.5}Ag_{3.5}$	580 ± 7	8.7 ± 0.9	7.48 ± 0.05	7.2 ± 0.8
$Sn_{97}Cu_3$	569 ± 8	7.6 ± 1.0	7.15 ± 0.07	4.0 ± 0.9
$Sn_{90}Pb_{10}$	543 ± 4	6.6 ± 0.5	7.54 ± 0.04	7.2 ± 0.6
$Sn_{60}Pb_{40}$	514 ± 2	7.1 ± 0.3	8.45 ± 0.02	7.6 ± 0.2

5. Summary

The surface tension and density of the liquid $Sn_{60}Pb_{40}$, $Sn_{90}Pb_{10}$, $Sn_{96.5}Ag_{3.5}$ and $Sn_{97}Cu_3$ solder alloys were determined over a wide temperature interval. The surface tension and the density of the alloys studied decrease with increasing temperature. The temperature dependences $\sigma(T)$ and $\rho(T)$ in the ranges investigated can be well approximated by linear functions. Comparison of the experimental data for the alloys studied shows that the reduction of the Pb content in the Sn–Pb soldering materials and, moreover, the change from Pb to Ag or Cu significantly increase the surface tension in the liquid state.

Acknowledgment

SM was supported within the framework of the European Cooperation in the field of Scientific and Technical Research—European Concerted Action on 'Lead-free Solder Materials' COST 531.

References

[1] Directive 2002/95/EC of the European Parliament and of the Council of 27 January 2003 on the restriction of the use of certain hazardous substances in electrical and electronic equipment *Official Journal of the European Union* 13.02.2003, L37/19
Directive 2002/96/EC of the European Parliament and of the Council of 27 January 2003 on waste electrical and electronic equipment (WEEE) *Official Journal of the European Union* 13.02.2003, L37/24
[2] Merkwitz M 1997 *PhD Thesis* Technische Universität Chemnitz http://archiv.tu-chemnitz.de/pub/1997/0036
[3] Merkwitz M, Weise J, Thriemer K and Hoyer W 1998 *Z. Metallk.* **89** 247
[4] Greiner W and Stock H 1984 *Theoretische Physik: Hydrodynamik* (Frankfurt a. M.: Harri Deutsch)
[5] De Gennes P-G, Brochard-Wyart F and Quéré D 2002 *Gouttes, Bulles, Perles et Ondes* (Paris: Belin)
[6] Kaban I, Gruner S and Hoyer W 2004 *12th Int. Conf. on Liquid and Amorphous Metals (Metz, France, July 2004)*; *J. Non-Cryst. Solids* Abstracts Book and Programme LAM12–K02, at press
[7] Bulwith R, Sitek J, Bukat K and Hozer L 2002 *Glob. SMT Packaging J.* **2/9** 16
[8] Moser Z, Gasior W and Pstrus J 2001 *J. Phase Equilib.* **22** 254
[9] Hoar T P and Milford D A 1957 *Trans. Faraday Soc.* **53** 315
[10] White D W G 1971 *Metall. Trans.* **2** 3067
[11] Caroll M A and Warwick M E 1987 *Mater. Sci. Technol.* **3** 1040
[12] Gasior W, Moser Z and Pstrus J 2001 *J. Phase Equilib.* **22** 20